

EXPERIMENTAL STUDY FOR IK AIRFOIL AT LOW SPEED IN A RECTANGULAR AIR CROSS FLOW

AMJED AL-KHATEEB¹, MOHAMMED K. KHASHAN¹ & ALI SH. BAQIR²

¹Department of Aeronautical Technologies, Najaf Technical Institute, Al-Furat Al-Awsat Technical University, Al-Najaf, Iraq

²Engineering Technical College/Najaf, Al-Furat Al-Awsat Technical University, Al-Najaf, Iraq

ABSTRACT

The airfoil design problem has played an important role since the man first expressed the desire to fly till now so as to adapt man's air plane application with a good aerodynamic performance requirements, including lift, drag and pitching moment in a specified Mach/ Reynold number flow regime as well as geometric constraints. Therefore, it would always be desirable to design an airfoil with the ability to adapt to its current flow conditions and alter its shape to keep it efficient at any speed. This work, based on designing and experimental investigation the ability of the new (IK) airfoil design to work in a wide range of subsonic speeds. The (IK)air foil cord length 157mm,span length 300mm, maximum thickness 10.32. The experiment covers the following ranges :Reynolds number 152908-305816 and angle of attack (-6°, -3°, 0°, 3°, 6°, 9°, 12°, 15°, 18°, 21°, 24° and 33°). Results showed that as speed increases lift coefficient increases to reach a max value (10.227) at Reynold number 264844 and attack angle (30°). The ratio of lift to drag coefficient (C_L/C_D) reaches its max value with the same Reynold number, but at an attack angle equals to (3°) where it reaches (10.0857), beyond this threshold (C_L) and (C_L/C_D) will start to decrease as speed increase.

KEYWORDS: Aerodynamic Enhancement, Angle of Attack, Drag Force Coefficient, IK Airfoil, Lift force Coefficient & Subsonic Wind Tunnel

Received: Dec 16, 2018; **Accepted:** Jan 06, 2019; **Published:** Feb 01, 2019; **Paper Id.:** IJMPERDAPR20191

INTRODUCTION

Work on the airfoil design problem originated as a response to a general question from A. M. O. Smith: "What is the maximum lift which can be obtained from an airfoil, and what is the shape of that airfoil?" Liebeck [1].

By the aid of mini-computer, a new airflow design method has been introduced and this can be used to measure the velocity distribution which will produce desired parameter (i. e. lift, drag and pitching moment) and test for boundary layer separation, Narramore [2].

Aerodynamic surface has a major role in providing the sufficient lift force to maintain the flight vehicle in the air while keeping the drag of the aerodynamic surface as low as possible. Therefore, measuring the change in aerodynamic forces due to airfield deformation in the wind tunnel is the best way to assess the feasibility of the proposed design, Leung [3].

A shock wave generation on the fighter aircraft wing is important in supersonic flight regime, so the appropriate airfoil design should be considered to lessen the wave drag produce by these shock waves. It is better to make the leading edge of the airfoil sharp in order to decrease the bow shock that occur in front of the blunt

edges in supersonic flying. As a result, double wedge airfoil would perform best in supersonic speed regime, but this would not be true at subsonic flight regime because of the sharp edge stall. For this purpose and to improve the performance characteristics of supersonic double wedge airfoil at low speed experimental study was done by modifying the diamond section shape to prepared flying in a wide range of different speed.

Supersonic airfoils such diamond section airfoil is the most efficient airfoils for supersonic aircraft at supersonic speed. This airfoil is common with a sharp leading edge and apexes to form oblique and expansion shocks which are responsible for the producing of the aerodynamic characteristics during flight at supersonic speed. These types of shocks reduced the wave drag more than for a bow shock that will be formed for a curvature leading edge airfoil. The distribution of pressure around a diamond section airfoil in the supersonic mode is very much simpler than that in the subsonic mode, each of the four faces of the diamond cross-section experiencing virtually constant pressure. **Mohammed I. Abutabikh, et. al, [4]** performed the diamond section airfoil in both supersonic and subsonic speed regime. The result showed good performance in the supersonic speed while poor performance at subsonic speed due to sharp edge stall. They're undertaken to improve the performance characteristics of the diamond section airfoil at low speeds by utilizing passive-active flow control methods. The passive method involved modifying the shape by changing the sharp leading edge and midsection upper and lower apex surface to a smooth curved control segment, while the active method involved blowing technique. **Barnard, et. al, [5]** analysis the shape, the sharpness of the supersonic airfoils and affect the aerodynamic characteristics in an undesirable manner with low speeds due to the separation of flow at leading edge and surfaces apexes which leads to a low lift coefficient, which intern demands.

There are many approaches to flow control proposed by researchers concerning the problem to improve the lift characteristics of supersonic airfoil at low speeds. **Pollok, et. al, [6]** presented a study of methods to increase the lift of a double wedge supersonic airfoils at low speeds. Their results indicate that the nose flap had an appreciable effect on preventing separation and thus increasing the lift and split flaps give an increment of lift as it would be expected, while blowing the boundary layer at the top surface improve lift and drag characteristics. **Bacon, [7]** investigated the blowing method as a means of rising the maximum lift of supersonic wings at low subsonic speeds and he concluded that the blowing method is promising to improve double wedge supersonic airfoil aerodynamic characteristics. **Miranda, et. al, [8]** performed active control of fully separated flow over a symmetrical circular-arc airfoil at high angle of attack. These tests were undertaken at low aped, open-circuit wind tunnel with attack angle between (10° - 40°). Low power input, unsteady excitation was applied to the leading or trailing edge. Measurements of pressure over the airfoil show that flow control increased the normal forces coefficient by up to 70%.

Mashud, et. al. [9] observed that the flow over sharp edged wings is almost always separated. The control of separated flows, not flow separation, is possible and benefits can be achieved, but only in a time average sense.

A new periodic blowing technique was designed and tested that can attain a wide range of velocities. In contrast to the traditional synthetic jet, the actuator is capable of producing a significant amount of jet vectoring and thus help to align the disturbance with the leading edge shear layer. The results showed that unsteady mini-jet actuation is an efficient device this is able to raise the lift in the airfoil stall region. In the present research, the interest is focused on the supersonic double wedge airfoil. This type of wing sections performs excellent at the supersonic speed regime has a poor performance at low speed as a result of the sharp edges stall. Therefore an experimental and theoretical study was undertaken to determine the double wedge airfoil performance improvement at low speed.

EXPERIMENTAL EQUIPMENT AND PROCEDURES

In this study, measurement of aerodynamic force was undertaken in the low-speed open circuit wind tunnel of Department of Aeronautical Engineering, Al-Furat Al-Awsat Technical University. Details of wind tunnel with assembled dimensions of about (3700 mm x 1065 mm x height 1900 mm and 293 kg weight) and with working section (305 mm x 305 mm, and 600 mm long), air velocity within (0 to 36) m. s⁻¹ and noise levels about 80 dB(A).

The lift and drag forces are measured by using the two component balance that is mounted in subsonic wind tunnel. The balance mechanism of lift/drag force equipment facilitate mounting of test models with a rigid support rod and hold airfoil or wing in position in the wind tunnel working section. The force on the test model is transmitted directly to a strain gauged load cell by the rod. The load cell is connected to a readout unit with a digital screen, which is turned through a socket power supply. In addition, the equipment Photographs of the wind tunnel, test section and lift/drag force equipment are presented in figure 1 and 2.

IK airfoil designed by using SOLIDWORKS program with geometry and shape shown in figure 3. By using 3-D printer a model of the airfoil was fabricated from polylactic acid (PLA) for the purpose of experiment the characteristics of IK airfoil by using in wind tunnel. IK airfoil was used in the test section with difference angles of attack and air flow velocities. The nomenclature and all parameter of IK airfoil test illustrated in Table 1. In the experiment, the Reynolds number range was 152908-305816, which is based on chord length. Angle of attack variation used in the experimental -6°, -3°, 0°, 3°, 6°, 9°, 12°, 15°, 18°, 21°, 24° and 33°. Air is the working fluid in the experiment. The air temperature for after and before test section side measures by K-thermocouples. Each run of experiments take 10 min even after the steady-state which is between 10-15 min. All the above equipment used for various measurements were calibrated.

The accuracy of all figures are estimated at (± 3.6 % accuracy of measured value for reading due to deformation, misused and uncertainty, ± 1.4 % for K type thermocouples).

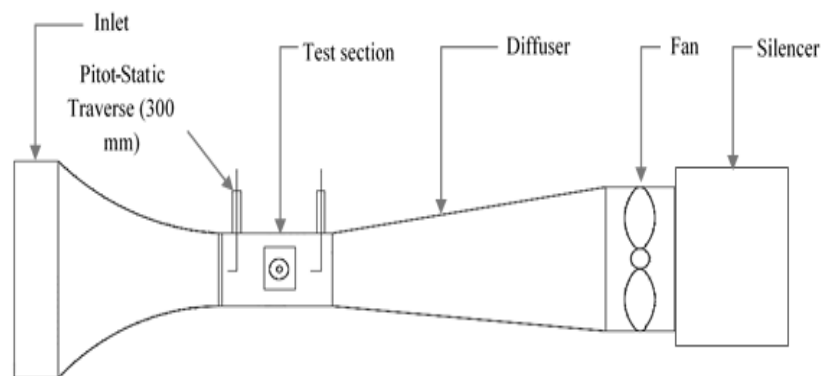


Figure 1: Schematic Diagram of the Wind Tunnel

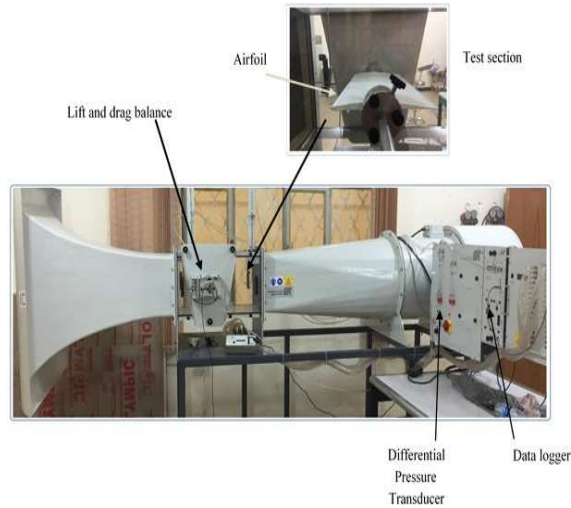


Figure 2: Photograph of the Wind Tunnel

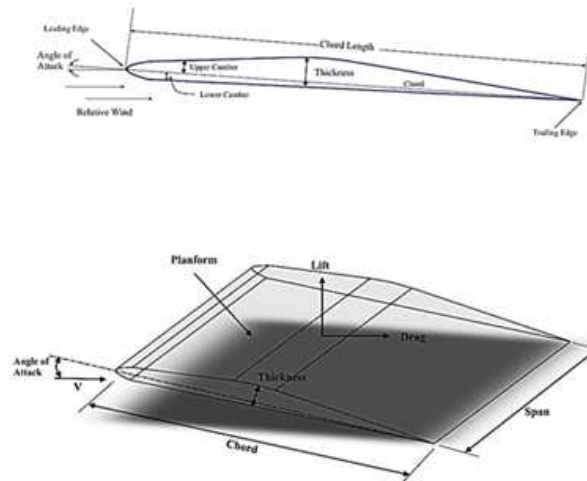


Figure 3: IK Airfoil Nomenclature

Table 1: IK Airfoil Parameters

Parameters	Symbol	Value
Chord	c	157 mm
Span	s	295 mm
Test Section Length	l	600 mm
Test Section Width	w	300 mm
Test Section depth	d	300 mm
Air Velocity	v	(0-36)m. s ⁻¹

Data Processing and Analysis

Bernoulli's Equation in eq.1, function of density, pressure, specific weight and velocity was used to calculate the air flow velocity along the streamline from Pitot tube as:

$$P_1 + \frac{1}{2}\rho V_1^2 = P_2 + \frac{1}{2}\rho V_2^2 \dots \quad (1)$$

where

P_1, P_2 are the total and static pressure,

V_1, V_2 are the total and static air flow velocity.

Eq. 1 rearranged to calculate the velocity along the streamline as written below;

$$V = \sqrt{2 \frac{\Delta P}{\rho}} \quad (2)$$

Where the pressure difference can be written as

$$\Delta P = \frac{1}{2} \rho V^2 \quad (3)$$

The lift force, L is a function of dynamic pressure, maximum projected wing or area surface area, A_s and lift coefficient, C_L as in the following equation;

$$L = \frac{1}{2} \rho_a V^2 A_s C_L \quad (4)$$

Where the surface area, A_s is calculated as follows;

$$A_s = c s \quad (5)$$

The drag force, D is a function of maximum projected wing or surface area, dynamic pressure and drag coefficient C_D as in the following equation;

$$D = \frac{1}{2} \rho_a V^2 A_s C_D \quad (6)$$

The dimensionless group Reynolds number, Re is calculated as follows;

$$Re = \frac{c V}{\nu} \quad (7)$$

Where ν is the kinematic viscosity $m^2 \cdot s^{-1}$

Uncertainty Analysis

The calculation of uncertainty is used in the present experimental processes and its refers to evaluate the error that may makes in the experimental processes A method of estimating uncertainty in present experimental results is calculated as follows for Re number as example;

$$w_{Re} = \left[\left(\frac{\partial Re}{\partial c} w_c \right)^2 + \left(\frac{\partial Re}{\partial u} w_u \right)^2 + \left(\frac{\partial Re}{\partial v} w_v \right)^2 \right]^{\frac{1}{2}} \quad (8)$$

Where

w_{Re} is the uncertainty of Re number, w_c , w_v and w_u are the uncertainty for independent variables.

RESULTS AND DISCUSSIONS

Figures (4-7) show the variation of Lift coefficient (C_L), Drag coefficient (C_D) and Lift to Drag ratio (C_L/C_D) with different of angle of attack and Reynolds number between 152908-305816. It's clearly shown that in figure 4 with Reynold number:152908 the lift is increasing when the angle of attack is increasing and the maximum lift coefficient (C_L) obtained at (15°) angle of attack where its reach (0.788). After this angle (C_L) is decreasing until (18°) and then return to increasing until it reach to (24°). Drag coefficient (C_D) is decreasing at (0°) angle of attack to its minimum value as (0.00722) and

then (C_D) is increasing with angle of attack increasing. The maximum value of lift to drag ratio (C_L/C_D) was obtain to be (4) at angle of attack equal (3°). Figure 5 with Reynold number:216244 show that lift is increasing when the angle of attack is increasing and the maximum lift coefficient (C_L) obtained at (24°) attack angle where its reach (0.0.938). lift coefficient (C_L) is decreasing slightly from (15°) until (18°) as seen in previously and then return to increasing until it reach to (24°). Drag coefficient (C_D) is decreasing at (0°) angle of attack to its minimum value as (0.00722) and then (C_D) is increasing with angle of attack increasing. The maximum value of lift to drag ratio (C_L/C_D) was obtain to be (4.4) at angle of attack equal (9°). From figure 6 with Reynold, number: 264844. it's clearly shown that the lift is increasing when the angle of attack is increasing and the maximum lift coefficient (C_L) obtained at (30°) angle of attack is (1.227). Drag coefficient (C_D) is decreasing at (0°) angle of attack to be the minimum value of (0.00819) and (C_D) is increasing with angle of attack increasing. The maximum value of lift to drag ratio (C_L/C_D) was obtain at (3°) angle of attack as (10.0857). Figure 7 with Reynold, number: 305816. it's clearly shown that the lift is increasing when the angle of attack is increasing but with values that lower in compare with the prior speed so it reach the maximum lift coefficient (C_L) at (27°) angle of attack was (0.9539). Drag coefficient (C_D) is decreasing at (0°) angle of attack to be the minimum value of (0.01806) and (C_D) is increasing with angle of attack increasing. The maximum value of lift to drag ratio (C_L/C_D) was obtain at (9°) angle of attack as (10.0321).

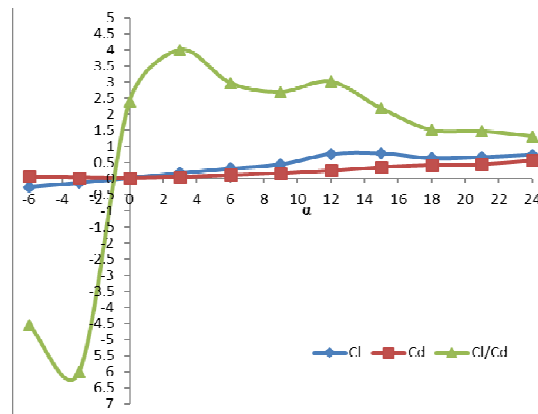


Figure 4: Lift Coefficient (C_L), Drag Coefficient (C_D) and Lift to Drag Ratio (C_L/C_D) with Angle of Attack $Re = 152908$

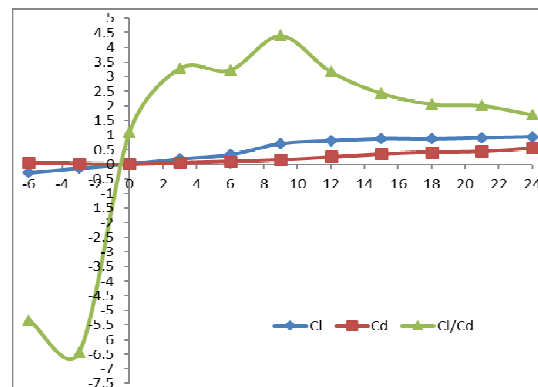


Figure 5: Lift Coefficient (C_L), Drag Coefficient (C_D) and Lift to Drag Ratio (C_L/C_D) with Angle of Attack at $Re = 216244$

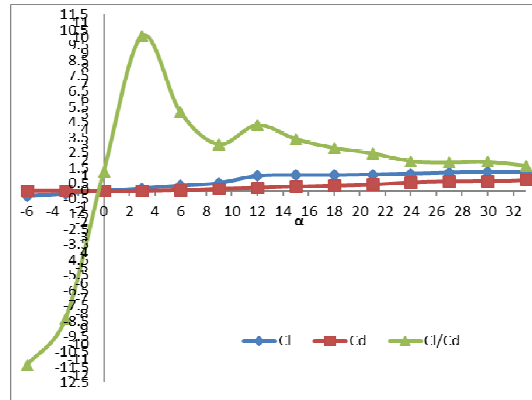


Figure 6: Lift Coefficient (C_L), Drag Coefficient (C_D) and Lift to Drag Ratio (C_L/C_D) with Angle of Attack at $Re = 264844$

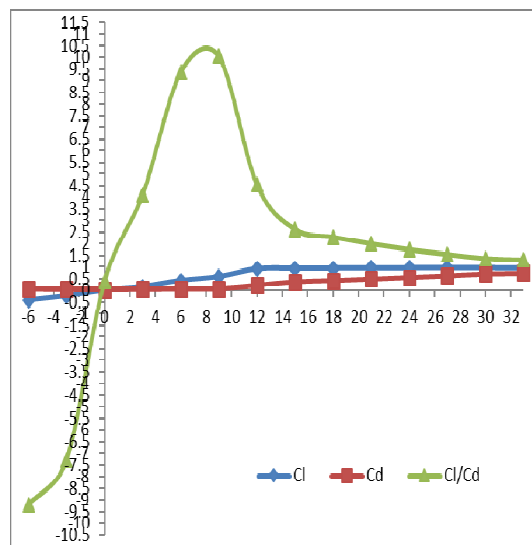


Figure 7: Lift Coefficient (C_L), Drag Coefficient (C_D) and Lift to Drag Ratio (C_L/C_D) with Angle of Attack at $Re = 305816$

CONCLUSIONS

The drag and lift force has been experimentally evaluated in the wind tunnel for the new airfield design (IK) to investigate its ability to work with a wide range of speed and angle of attack. According to the result, the following useful conclusion can be made. :

- In general lift coefficient increase as the attack angle increase, also lift coefficient increase with speed increase for the first three speeds when it's been to slightly decrease with forth one.
- Lift coefficient with the first three speed show a slight decrease in between (15° - 18°) angle of attack accept with forth with Reynold number 305816 where it continues to increase
- The maximum value of lift to drag coefficient obtained in attack angle (3°) with Reynold number 1520908 and 264844 while its max value with Reynold number 216244 and 305816 was reached at (9°) angle of attack
- Drag coefficient reaches its minimum value in all speed with the same angle of attack (0°)

- Max lift to drag coefficient was reached with Reynold number 265844 where it reach (10.0857) at an angle of attack (3°)

REFERENCES

1. Robert H. Liebeck, "Design of Subsonic Airfoils for High Lift" *Fluid and Plasma Dynamics Conference, San Diego, Calif., Vol. 15, No. 9, SEPTEMBER 1978. pp 547-561*
2. J. C. Narramore "An Approach to Subsonic, Turbulent Flow Airfoil Design Using Mini-Computers" *Society of Automotive Engineers, Inc. 1978. pp 2018-2026*
3. R. C. K. Leung, "Design of Shape Memory Alloy Actuated Deformable Airfoil for Subsonic Flight" *Key Engineering Materials Vols 334-335 (2007) pp 1105-1108*
4. Mohammed I. Abutabikh, Abdul Kareem A. Al-musawi and Mohammed K. Khashan. "Improving the Lift Characteristics of Supersonic Double Wedge Airfoil at Low Speed Using Passive-Active Flow Controlling Methods", *Mechanical Engineering Department, University of technology, Baghdad, Iraq, Engineering and Technical Journal, Vol 33, Part (A), No.1, 2015*
5. Basu, S., Singh, R. K., Anwar, A. S., & Rohit, B. *Influence Of Wingtip Devices In Reducing Induced Drag-A Review.*
6. R. H. Barnard, and D. R. Philpott, "Aircraft Flight", Vol. 4, PP 215-223, 2010.
7. Pollok, A. D. & Reck, F. F. "A Study of Method to Increase the Lift of Supersonic at Low Speed", Thesis, California Institute of technology, Pasadena, California 1947.
8. Bacon, J. W. Jr. "An Investigation of Blowing as a Method of Increasing the Maximum Lift of a Double Wedge Airfoil", Thesis, California Institute of technology, Pasadena, California 1949.
9. Serio Miranda, Pavlos P. Vlachos, Demetri P. Telionis, and Matthew D. Zeiger. "Flow control of a sharp-edged airfoil", *Virginia Polytechnic Institute and state university, Blacksburg, Virginia, AIAA journal, VOL 43, No.4 (2005), pp. 716-726, 2005.*
10. Sreelakshmi, K., & Niharika, B. (2018). *Design and Analysis of mini-UAV. International Journal of Mechanical and Production Engineering Research and Development (IJMPERD), 8(1), 1-8.*
11. Mohammad Mashud, Md. Mahfuz Sarwar, Md. Abdul Ghani Mollah and Md. Farhad Hossain. "Experimental study of Separated Flow Control Over a Sharp-edged Arc Airfoil", *Department of Mechanical Engineering Khulna University of Engineering & Technology, Khulna, Bangladesh, International Journal of Engineering & Technology IJET-IJENS Vol 09, No.10, 2009.*

Appendix A

Uncertainty Example For $R_e = 152908.1487$ Computation the uncertainty in the Reynolds number is as follows:

$$R_e = \frac{c u}{v} \quad R_e = 152908.1487$$

$$c = 0.157 \pm 4 \times 10^{-4} \text{ m} \quad w_c = 4 \times 10^{-4} \text{ m}$$

$$u = 16.05 \pm 0.2 \text{ m/sec} \quad w_u = 0.2 \text{ m/sec}$$

$$v = 1.648 \times 10^{-5} \pm \frac{13.7 \times 10^{-8} \text{ m}^2}{\text{sec}}$$

$$w_v = 13.7 \times 10^{-8} \text{ m}^2/\text{sec}$$

$$\frac{\partial R_e}{\partial c} = \frac{u}{v} \frac{\partial R_e}{\partial c} = \frac{16.05}{1.648 \times 10^{-5}} = 9.74 \times 10^5$$

$$\frac{\partial R_e}{\partial u} = \frac{c}{v} \frac{\partial R_e}{\partial u} = \frac{0.157}{1.648 \times 10^{-5}} = 0.09526 \times 10^5$$

$$\frac{\partial R_e}{\partial \theta} = \frac{-c u}{v^2}$$

$$\frac{\partial R_e}{\partial v} = -\frac{0.157 \times 16.05}{1.648 \times 10^{-5}} = -1.648 \times 10^{10}$$

$$w_{R_e} = \left[\left(\frac{\partial R_e}{\partial c} w_c \right)^2 + \left(\frac{\partial R_e}{\partial u} w_u \right)^2 + \left(\frac{\partial R_e}{\partial v} w_v \right)^2 \right]^{\frac{1}{2}}$$

$$w_{R_e} = \left[\begin{array}{l} ((9.74 \times 10^5) \times 4 \times 10^{-4})^2 + \\ ((0.09526 \times 10^5) \times 0.2)^2 + \\ ((-1.648 \times 10^{10}) \times 13.7 \times 10^{-8})^2 \end{array} \right]^{\frac{1}{2}}$$

$$w_{R_e} = 2987 \text{ or } w_{R_e} = 1.94\%$$

